

This is the accepted manuscript made available via CHORUS. The article has been published as:

Measurement of the Proton-Air Cross Section at $\sqrt{s}=57$ TeV with the Pierre Auger Observatory

P. Abreu *et al.* (The Pierre Auger Collaboration)

Phys. Rev. Lett. **109**, 062002 — Published 10 August 2012

DOI: [10.1103/PhysRevLett.109.062002](https://doi.org/10.1103/PhysRevLett.109.062002)

Measurement of the proton-air cross-section at $\sqrt{s} = 57$ TeV with the Pierre Auger Observatory

P. Abreu,¹ M. Aglietta,² E.J. Ahn,³ I.F.M. Albuquerque,⁴ D. Allard,⁵ I. Allekotte,⁶ J. Allen,⁷ P. Allison,⁸ A. Almeda,^{9,10} J. Alvarez Castillo,¹¹ J. Alvarez-Muñiz,¹² M. Ambrosio,¹³ A. Aminaei,¹⁴ L. Anchordoqui,¹⁵ S. Andringa,¹ T. Antićić,¹⁶ C. Aramo,¹³ E. Arganda,^{17,18} F. Arqueros,¹⁸ H. Asorey,⁶ P. Assis,¹ J. Aublin,¹⁹ M. Ave,²⁰ M. Avenier,²¹ G. Avila,²² T. Bäcker,²³ M. Balzer,²⁴ K.B. Barber,²⁵ A.F. Barbosa,²⁶ R. Bardenet,²⁷ S.L.C. Barroso,²⁸ B. Baughman,⁸ J. Bäuml,²⁹ J.J. Beatty,⁸ B.R. Becker,³⁰ K.H. Becker,³¹ A. Bellétoile,³² J.A. Bellido,²⁵ S. BenZvi,³³ C. Berat,²¹ X. Bertou,⁶ P.L. Biermann,³⁴ P. Billoir,¹⁹ F. Blanco,¹⁸ M. Blanco,³⁵ C. Bleve,³¹ H. Blümmer,^{20,29} M. Boháčová,³⁶ D. Boncioli,³⁷ C. Bonifazi,^{38,19} R. Bonino,² N. Borodai,³⁹ J. Brack,⁴⁰ P. Brogueira,¹ W.C. Brown,⁴¹ R. Bruijn,⁴² P. Buchholz,²³ A. Bueno,⁴³ R.E. Burton,⁴⁴ K.S. Caballero-Mora,⁴⁵ L. Caramete,³⁴ R. Caruso,⁴⁶ A. Castellina,² O. Catalano,⁴⁷ G. Cataldi,⁴⁸ L. Cazon,¹ R. Cester,⁴⁹ J. Chauvin,²¹ S.H. Cheng,⁴⁵ A. Chiavassa,² J.A. Chinellato,⁵⁰ J. Chirinos Diaz,⁵¹ J. Chudoba,³⁶ R.W. Clay,²⁵ M.R. Coluccia,⁴⁸ R. Conceição,¹ F. Contreras,⁵² H. Cook,⁴² M.J. Cooper,²⁵ J. Coppens,^{14,53} A. Cordier,²⁷ S. Coutu,⁴⁵ C.E. Covault,⁴⁴ A. Creusot,^{5,54} A. Criss,⁴⁵ J. Cronin,⁵⁵ A. Curutiu,³⁴ S. Dagoret-Campagne,²⁷ R. Dallier,³² S. Dasso,^{56,57} K. Daumiller,²⁹ B.R. Dawson,²⁵ R.M. de Almeida,⁵⁸ M. De Domenico,⁴⁶ C. De Donato,¹¹ S.J. de Jong,^{14,53} G. De La Vega,⁵⁹ W.J.M. de Mello Junior,⁵⁰ J.R.T. de Mello Neto,³⁸ I. De Mitri,⁴⁸ V. de Souza,⁶⁰ K.D. de Vries,⁶¹ G. Decerprit,⁵ L. del Peral,³⁵ M. del Río,^{37,52} O. Deligny,⁶² H. Dembinski,²⁰ N. Dhital,⁵¹ C. Di Giulio,⁶³ M.L. Díaz Castro,⁶⁴ P.N. Diep,⁶⁵ C. Dobrigkeit,⁵⁰ W. Docters,⁶¹ J.C. D'Olivo,¹¹ P.N. Dong,^{65,62} A. Dorofeev,⁴⁰ J.C. dos Anjos,²⁶ M.T. Dova,¹⁷ D. D'Urso,¹³ I. Dutan,³⁴ J. Ebr,³⁶ R. Engel,²⁹ M. Erdmann,⁶⁶ C.O. Escobar,⁵⁰ J. Espadanal,¹ A. Etchegoyen,^{10,9} P. Facal San Luis,⁵⁵ I. Fajardo Tapia,¹¹ H. Falcke,^{14,67} G. Farrar,⁷ A.C. Fauth,⁵⁰ N. Fazzini,³ A.P. Ferguson,⁴⁴ A. Ferrero,¹⁰ B. Fick,⁵¹ A. Filevich,¹⁰ A. Filipčič,^{68,54} S. Fliescher,⁶⁶ C.E. Fracchiolla,⁴⁰ E.D. Fraenkel,⁶¹ U. Fröhlich,²³ B. Fuchs,²⁶ R. Gaior,¹⁹ R.F. Gamarra,¹⁰ S. Gambetta,⁶⁹ B. García,⁵⁹ D. Garcia-Gomez,²⁷ D. Garcia-Pinto,¹⁸ A. Gascon,⁴³ H. Gemmeke,²⁴ K. Gesterling,³⁰ P.L. Ghia,^{19,2} U. Giaccari,⁴⁸ M. Giller,⁷⁰ H. Glass,³ M.S. Gold,³⁰ G. Golup,⁶ F. Gomez Albarracin,¹⁷ M. Gómez Berisso,⁶ P. Gonçalves,¹ D. Gonzalez,²⁰ J.G. Gonzalez,²⁰ B. Gookin,⁴⁰ D. Góra,^{20,39} A. Gorgi,² P. Gouffon,⁴ S.R. Gozzini,⁴² E. Grashorn,⁸ S. Grebe,^{14,53} N. Griffith,⁸ M. Grigat,⁶⁶ A.F. Grillo,⁷¹ Y. Guardincerri,⁵⁷ F. Guarino,¹³ G.P. Guedes,⁷² A. Guzman,¹¹ J.D. Hague,³⁰ P. Hansen,¹⁷ D. Harari,⁶ S. Harmsma,^{61,53} T.A. Harrison,²⁵ J.L. Harton,⁴⁰ A. Haungs,²⁹ T. Hebbeker,⁶⁶ D. Heck,²⁹ A.E. Herve,²⁵ C. Hojvat,³ N. Hollon,⁵⁵ V.C. Holmes,²⁵ P. Homola,³⁹ J.R. Hörandel,¹⁴ A. Horneffer,¹⁴ P. Horvath,⁷³ M. Hrabovský,^{73,36} T. Huege,²⁹ A. Insolia,⁴⁶ F. Ionita,⁵⁵ A. Italiano,⁴⁶ C. Jarne,¹⁷ S. Jiraskova,¹⁴ M. Josebachuili,¹⁰ K. Kadja,¹⁶ K.H. Kampert,³¹ P. Karhan,⁷⁴ P. Kasper,³ B. Kégl,²⁷ B. Keilhauer,²⁹ A. Keivani,⁷⁵ J.L. Kelley,¹⁴ E. Kemp,⁵⁰ R.M. Kieckhafer,⁵¹ H.O. Klages,²⁹ M. Kleifges,²⁴ J. Kleinfeller,²⁹ J. Knapp,⁴² D.-H. Koang,²¹ K. Kotera,⁵⁵ N. Krohm,³¹ O. Krömer,²⁴ D. Kruppke-Hansen,³¹ F. Kuehn,³ D. Kuempel,³¹ J.K. Kulbartz,⁷⁶ N. Kunka,²⁴ G. La Rosa,⁴⁷ C. Lachaud,⁵ R. Lauer,³⁰ P. Lautridou,³² S. Le Coz,²¹ M.S.A.B. Leão,⁷⁷ D. Lebrun,²¹ P. Lebrun,³ M.A. Leigui de Oliveira,⁷⁷ A. Lemiere,⁶² A. Letessier-Selvon,¹⁹ I. Lhenry-Yvon,⁶² K. Link,²⁰ R. López,⁷⁸ A. Lopez Agüera,¹² K. Louedec,^{21,27} J. Lozano Bahilo,⁴³ L. Lu,⁴² A. Lucero,^{10,2} M. Ludwig,²⁰ H. Lyberis,⁶² C. Macolino,¹⁹ S. Maldera,² D. Mandat,³⁶ P. Mantsch,³ A.G. Mariazzi,¹⁷ J. Marin,^{52,2} V. Marin,³² I.C. Maris,¹⁹ H.R. Marquez Falcon,⁷⁹ G. Marsella,⁸⁰ D. Martello,⁴⁸ L. Martin,³² H. Martinez,⁸¹ O. Martínez Bravo,⁷⁸ H.J. Mathes,²⁹ J. Matthews,^{75,82} J.A.J. Matthews,³⁰ G. Matthiae,³⁷ D. Maurizio,⁴⁹ P.O. Mazur,³ G. Medina-Tanco,¹¹ M. Melissas,²⁰ D. Melo,^{10,49} E. Menichetti,⁴⁹ A. Menshikov,²⁴ P. Mertsch,⁸³ C. Meurer,⁶⁶ S. Mićanović,¹⁶ M.I. Micheletti,⁸⁴ W. Miller,³⁰ L. Miramonti,⁸⁵ L. Molina-Bueno,⁴³ S. Mollerach,⁶ M. Monasor,⁵⁵ D. Monnier Ragaigne,²⁷ F. Montanet,²¹ B. Morales,¹¹ C. Morello,² E. Moreno,⁷⁸ J.C. Moreno,¹⁷ C. Morris,⁸ M. Mostafá,⁴⁰ C.A. Moura,^{77,13} S. Mueller,²⁹ M.A. Muller,⁵⁰ G. Müller,⁶⁶ M. Müncihmeyer,¹⁹ R. Mussa,⁴⁹ G. Navarra,² J.L. Navarro,⁴³ S. Navas,⁴³ P. Necesal,³⁶ L. Nellen,¹¹ A. Nelles,^{14,53} J. Neuser,³¹ P.T. Nhung,⁶⁵ L. Niemietz,³¹ N. Nierstenhoefer,³¹ D. Nitz,⁵¹ D. Nosek,⁷⁴ L. Nožka,³⁶ M. Nyklicek,³⁶ J. Oehlschläger,²⁹ A. Olinto,⁵⁵ V.M. Olmos-Gilbaja,¹² M. Ortiz,¹⁸ N. Pacheco,³⁵ D. Pakk Selmi-Dei,⁵⁰ M. Palatka,³⁶ J. Pallotta,⁸⁶ N. Palmieri,²⁰ G. Parente,¹² E. Parizot,⁵ A. Parra,¹² R.D. Parsons,⁴² S. Pastor,⁸⁷ T. Paul,⁸⁸ M. Pech,³⁶ J. Pękala,³⁹ R. Pelayo,^{78,12} I.M. Pepe,⁸⁹ L. Perrone,⁸⁰ R. Pesce,⁶⁹ E. Petermann,⁹⁰ S. Petrera,⁶³ P. Petrinca,³⁷ A. Petrolini,⁶⁹ Y. Petrov,⁴⁰ J. Petrovic,⁵³ C. Pfendner,³³ N. Phan,³⁰ R. Piegaia,⁵⁷ T. Pierog,²⁹ P. Pieroni,⁵⁷ M. Pimenta,¹ V. Pirronello,⁴⁶ M. Platino,¹⁰ V.H. Ponce,⁶ M. Pontz,²³ P. Privitera,⁵⁵ M. Prouza,³⁶ E.J. Quel,⁸⁶ S. Querchfeld,³¹ J. Rautenberg,³¹ O. Ravel,³² D. Ravignani,¹⁰

B. Revenu,³² J. Ridky,³⁶ S. Riggi,^{12,46} M. Risse,²³ P. Ristori,⁸⁶ H. Rivera,⁸⁵ V. Rizi,⁶³ J. Roberts,⁷ C. Robledo,⁷⁸ W. Rodrigues de Carvalho,^{12,4} G. Rodriguez,¹² J. Rodriguez Martino,⁵² J. Rodriguez Rojo,⁵² I. Rodriguez-Cabo,¹² M.D. Rodriguez-Frías,³⁵ G. Ros,³⁵ J. Rosado,¹⁸ T. Rossler,⁷³ M. Roth,²⁹ B. Rouillé-d'Orfeuil,⁵⁵ E. Roulet,⁶ A.C. Rovero,⁵⁶ C. Rühle,²⁴ F. Salamida,^{62,63} H. Salazar,⁷⁸ F. Salesa Greus,⁴⁰ G. Salina,³⁷ F. Sánchez,¹⁰ C.E. Santo,¹ E. Santos,¹ E.M. Santos,³⁸ F. Sarazin,⁹¹ B. Sarkar,³¹ S. Sarkar,⁸³ R. Sato,⁵² N. Scharf,⁶⁶ V. Scherini,⁸⁵ H. Schieler,²⁹ P. Schiffer,^{76,66} A. Schmidt,²⁴ O. Scholten,⁶¹ H. Schoorlemmer,^{14,53} J. Schovancova,³⁶ P. Schovánek,³⁶ F. Schröder,²⁹ S. Schulte,⁶⁶ D. Schuster,⁹¹ S.J. Sciutto,¹⁷ M. Scuderi,⁴⁶ A. Segreto,⁴⁷ M. Settimo,²³ A. Shadkam,⁷⁵ R.C. Shellard,^{26,64} I. Sidelnik,¹⁰ G. Sigl,⁷⁶ H.H. Silva Lopez,¹¹ A. Śmialkowski,⁷⁰ R. Šmídá,^{29,36} G.R. Snow,⁹⁰ P. Sommers,⁴⁵ J. Sorokin,²⁵ H. Spinka,^{92,3} R. Squartini,⁵² S. Stanic,⁵⁴ J. Stapleton,⁸ J. Stasielak,³⁹ M. Stephan,⁶⁶ A. Stutz,²¹ F. Suarez,¹⁰ T. Suomijärvi,⁶² A.D. Supanitsky,^{56,11} T. Šuša,¹⁶ M.S. Sutherland,^{75,8} J. Swain,⁸⁸ Z. Szadkowski,⁷⁰ M. Szuba,²⁹ A. Tamashiro,⁵⁶ A. Tapia,¹⁰ M. Tartare,²¹ O. Taşcău,³¹ C.G. Tavera Ruiz,¹¹ R. Tcaciuc,²³ D. Tegolo,^{46,93} N.T. Thao,⁶⁵ D. Thomas,⁴⁰ J. Tiffenberg,⁵⁷ C. Timmermans,^{53,14} D.K. Tiwari,⁷⁹ W. Tkaczyk,⁷⁰ C.J. Todero Peixoto,^{60,77} B. Tomé,¹ A. Tonachini,⁴⁹ P. Travnicek,³⁶ D.B. Tridapalli,⁴ G. Tristram,⁵ E. Trovato,⁴⁶ M. Tueros,^{12,57} R. Ulrich,^{29,45} M. Unger,²⁹ M. Urban,²⁷ J.F. Valdés Galicia,¹¹ I. Valiño,¹² L. Valore,¹³ A.M. van den Berg,⁶¹ E. Varela,⁷⁸ B. Vargas Cárdenas,¹¹ J.R. Vázquez,¹⁸ R.A. Vázquez,¹² D. Veberič,^{54,68} V. Verzi,³⁷ J. Vicha,³⁶ M. Videla,⁵⁹ L. Villaseñor,⁷⁹ H. Wahlberg,¹⁷ P. Wahrlich,²⁵ O. Wainberg,^{10,9} D. Walz,⁶⁶ D. Warner,⁴⁰ A.A. Watson,⁴² M. Weber,²⁴ K. Weidenhaupt,⁶⁶ A. Weindl,²⁹ S. Westerhoff,³³ B.J. Whelan,²⁵ G. Wieczorek,⁷⁰ L. Wiencke,⁹¹ B. Wilczyńska,³⁹ H. Wilczyński,³⁹ M. Will,²⁹ C. Williams,⁵⁵ T. Winchen,⁶⁶ M.G. Winnick,²⁵ M. Wommer,²⁹ B. Wundheiler,¹⁰ T. Yamamoto,⁵⁵ T. Yapici,⁵¹ P. Younk,^{23,94} G. Yuan,⁷⁵ A. Yushkov,^{12,13} B. Zamorano,⁴³ E. Zas,¹² D. Zavrtanik,^{54,68} M. Zavrtanik,^{68,54} I. Zaw,⁷ A. Zepeda,⁸¹ Y. Zhu,²⁴ M. Zimbres Silva,^{31,50} and M. Ziolkowski²³

(The Pierre Auger Collaboration)

¹LIP and Instituto Superior Técnico, Technical University of Lisbon, Portugal

²Istituto di Fisica dello Spazio Interplanetario (INAF),

Università di Torino and Sezione INFN, Torino, Italy

³Fermilab, Batavia, IL, USA

⁴Universidade de São Paulo, Instituto de Física, São Paulo, SP, Brazil

⁵Laboratoire AstroParticule et Cosmologie (APC),

Université Paris 7, CNRS-IN2P3, Paris, France

⁶Centro Atómico Bariloche and Instituto Balseiro (CNEA-UNCuyo-CONICET), San Carlos de Bariloche, Argentina

⁷New York University, New York, NY, USA

⁸Ohio State University, Columbus, OH, USA

⁹Universidad Tecnológica Nacional - Facultad Regional Buenos Aires, Buenos Aires, Argentina

¹⁰Instituto de Tecnologías en Detección y Astropartículas (CNEA, CONICET, UNSAM), Buenos Aires, Argentina

¹¹Universidad Nacional Autónoma de México, Mexico, D.F., Mexico

¹²Universidad de Santiago de Compostela, Spain

¹³Università di Napoli "Federico II" and Sezione INFN, Napoli, Italy

¹⁴IMAPP, Radboud University Nijmegen, Netherlands

¹⁵University of Wisconsin, Milwaukee, WI, USA

¹⁶Rudjer Bošković Institute, 10000 Zagreb, Croatia

¹⁷IFLP, Universidad Nacional de La Plata and CONICET, La Plata, Argentina

¹⁸Universidad Complutense de Madrid, Madrid, Spain

¹⁹Laboratoire de Physique Nucléaire et de Hautes Energies (LPNHE),

Universités Paris 6 et Paris 7, CNRS-IN2P3, Paris, France

²⁰Karlsruhe Institute of Technology - Campus South - Institut für Experimentelle Kernphysik (IEKP), Karlsruhe, Germany

²¹Laboratoire de Physique Subatomique et de Cosmologie (LPSC),

Université Joseph Fourier, INPG, CNRS-IN2P3, Grenoble, France

²²Observatorio Pierre Auger and Comisión Nacional de Energía Atómica, Malargüe, Argentina

²³Universität Siegen, Siegen, Germany

²⁴Karlsruhe Institute of Technology - Campus North - Institut für Prozessdatenverarbeitung und Elektronik, Karlsruhe, Germany

²⁵University of Adelaide, Adelaide, S.A., Australia

²⁶Centro Brasileiro de Pesquisas Fisicas, Rio de Janeiro, RJ, Brazil

²⁷Laboratoire de l'Accélérateur Linéaire (LAL), Université Paris 11, CNRS-IN2P3, Orsay, France

²⁸Universidade Estadual do Sudoeste da Bahia, Vitoria da Conquista, BA, Brazil

²⁹Karlsruhe Institute of Technology - Campus North - Institut für Kernphysik, Karlsruhe, Germany

³⁰University of New Mexico, Albuquerque, NM, USA

³¹Bergische Universität Wuppertal, Wuppertal, Germany

³²SUBATECH, École des Mines de Nantes, CNRS-IN2P3, Université de Nantes, Nantes, France

- ³³University of Wisconsin, Madison, WI, USA
³⁴Max-Planck-Institut für Radioastronomie, Bonn, Germany
³⁵Universidad de Alcalá, Alcalá de Henares (Madrid), Spain
³⁶Institute of Physics of the Academy of Sciences of the Czech Republic, Prague, Czech Republic
³⁷Università di Roma II "Tor Vergata" and Sezione INFN, Roma, Italy
³⁸Universidade Federal do Rio de Janeiro, Instituto de Física, Rio de Janeiro, RJ, Brazil
³⁹Institute of Nuclear Physics PAN, Krakow, Poland
⁴⁰Colorado State University, Fort Collins, CO, USA
⁴¹Colorado State University, Pueblo, CO, USA
⁴²School of Physics and Astronomy, University of Leeds, United Kingdom
⁴³Universidad de Granada & C.A.F.P.E., Granada, Spain
⁴⁴Case Western Reserve University, Cleveland, OH, USA
⁴⁵Pennsylvania State University, University Park, PA, USA
⁴⁶Università di Catania and Sezione INFN, Catania, Italy
⁴⁷Istituto di Astrofisica Spaziale e Fisica Cosmica di Palermo (INAF), Palermo, Italy
⁴⁸Dipartimento di Fisica dell'Università del Salento and Sezione INFN, Lecce, Italy
⁴⁹Università di Torino and Sezione INFN, Torino, Italy
⁵⁰Universidade Estadual de Campinas, IFGW, Campinas, SP, Brazil
⁵¹Michigan Technological University, Houghton, MI, USA
⁵²Observatorio Pierre Auger, Malargüe, Argentina
⁵³Nikhef, Science Park, Amsterdam, Netherlands
⁵⁴Laboratory for Astroparticle Physics, University of Nova Gorica, Slovenia
⁵⁵University of Chicago, Enrico Fermi Institute, Chicago, IL, USA
⁵⁶Instituto de Astronomía y Física del Espacio (CONICET-UBA), Buenos Aires, Argentina
⁵⁷Departamento de Física, FCEyN, Universidad de Buenos Aires y CONICET, Argentina
⁵⁸Universidade Federal Fluminense, EEIMVR, Volta Redonda, RJ, Brazil
⁵⁹National Technological University, Faculty Mendoza (CONICET/CNEA), Mendoza, Argentina
⁶⁰Universidade de São Paulo, Instituto de Física, São Carlos, SP, Brazil
⁶¹Kernfysisch Versneller Instituut, University of Groningen, Groningen, Netherlands
⁶²Institut de Physique Nucléaire d'Orsay (IPNO),
Université Paris 11, CNRS-IN2P3, Orsay, France
⁶³Università dell'Aquila and INFN, L'Aquila, Italy
⁶⁴Pontifícia Universidade Católica, Rio de Janeiro, RJ, Brazil
⁶⁵Institute for Nuclear Science and Technology (INST), Hanoi, Vietnam
⁶⁶RWTH Aachen University, III. Physikalisches Institut A, Aachen, Germany
⁶⁷ASTRON, Dwingeloo, Netherlands
⁶⁸J. Stefan Institute, Ljubljana, Slovenia
⁶⁹Dipartimento di Fisica dell'Università and INFN, Genova, Italy
⁷⁰University of Lódź, Lódź, Poland
⁷¹INFN, Laboratori Nazionali del Gran Sasso, Assergi (L'Aquila), Italy
⁷²Universidade Estadual de Feira de Santana, Brazil
⁷³Palacky University, RCPTM, Olomouc, Czech Republic
⁷⁴Charles University, Faculty of Mathematics and Physics,
Institute of Particle and Nuclear Physics, Prague, Czech Republic
⁷⁵Louisiana State University, Baton Rouge, LA, USA
⁷⁶Universität Hamburg, Hamburg, Germany
⁷⁷Universidade Federal do ABC, Santo André, SP, Brazil
⁷⁸Benemérita Universidad Autónoma de Puebla, Puebla, Mexico
⁷⁹Universidad Michoacana de San Nicolas de Hidalgo, Morelia, Michoacan, Mexico
⁸⁰Dipartimento di Ingegneria dell'Innovazione dell'Università del Salento and Sezione INFN, Lecce, Italy
⁸¹Centro de Investigación y de Estudios Avanzados del IPN (CINVESTAV), México, D.F., Mexico
⁸²Southern University, Baton Rouge, LA, USA
⁸³Rudolf Peierls Centre for Theoretical Physics, University of Oxford, Oxford, United Kingdom
⁸⁴Instituto de Física de Rosario (IFIR) - CONICET/U.N.R. and Facultad
de Ciencias Bioquímicas y Farmacéuticas U.N.R., Rosario, Argentina
⁸⁵Università di Milano and Sezione INFN, Milan, Italy
⁸⁶Centro de Investigaciones en Láseres y Aplicaciones, CITEFA and CONICET, Argentina
⁸⁷Instituto de Física Corpuscular, CSIC-Universitat de València, Valencia, Spain
⁸⁸Northeastern University, Boston, MA, USA
⁸⁹Universidade Federal da Bahia, Salvador, BA, Brazil
⁹⁰University of Nebraska, Lincoln, NE, USA
⁹¹Colorado School of Mines, Golden, CO, USA
⁹²Argonne National Laboratory, Argonne, IL, USA
⁹³Università di Palermo and Sezione INFN, Catania, Italy

⁹⁴*Los Alamos National Laboratory, Los Alamos, NM, USA*

We report a measurement of the proton-air cross-section for particle production at the center-of-mass energy per nucleon of 57 TeV. This is derived from the distribution of the depths of shower maxima observed with the Pierre Auger Observatory: systematic uncertainties are studied in detail. Analysing the tail of the distribution of the shower maxima, a proton-air cross-section of $[505 \pm 22(\text{stat})^{+28}_{-36}(\text{sys})]$ mb is found.

PACS numbers:

INTRODUCTION

We present the first analysis of the proton-air cross-section based on measurements made at the Pierre Auger Observatory [1]. For this purpose we analyse the shape of the distribution of the largest values of the depth of shower maximum, X_{\max} , the position at which an air shower deposits the maximum energy per unit of mass of atmosphere traversed. The *tail* of the X_{\max} -distribution is sensitive to the proton-air cross-section, a fact first exploited in the pioneering work of the Fly's Eye Collaboration [2]. To obtain accurate measurements of X_{\max} , timing data from the fluorescence telescopes is combined with that from the surface detector array for a precise hybrid reconstruction of the geometry of events [3].

We place particular emphasis on studying systematic uncertainties in the cross-section analysis. The unknown mass composition of cosmic-rays [4] is identified to be the major source of systematic uncertainty and accordingly the analysis has been optimised to minimise the impact of particles other than protons in the primary beam. This begins with restricting the analysis to the energy interval 10^{18} to $10^{18.5}$ eV, where the shape of the X_{\max} -distribution is compatible with there being a substantial fraction of protons; also there are a large number of events recorded in this energy range. The corresponding average center-of-mass energy of a proton interacting with a nucleon is 57 TeV, significantly above the reach of the Large Hadron Collider.

ANALYSIS APPROACH

The proton-air cross-section is derived in a two-step process. Firstly, we measure an air-shower observable with high sensitivity to the cross-section. Secondly, we convert this measurement to a value of the proton-air cross-section for particle production (c.f. [5]). This is the cross-section that accounts for all interactions which produce particles and thus contribute to the air-shower development; it implicitly also includes diffractive interactions. As the primary observable we define Λ_η via the exponential shape of the tail of the X_{\max} -distribution, $dN/dX_{\max} \propto \exp(-X_{\max}/\Lambda_\eta)$, where η denotes the fraction of most deeply penetrating air showers used. Considering only these events enhances the contribution of

protons in the sample, since the depth at which proton-induced showers maximise is deeper in the atmosphere than for showers from heavier nuclei. Thus, η is a key parameter: a small value enhances the proton fraction, but reduces the number of events available for the analysis. We have chosen $\eta = 0.2$ so that, for helium-fractions up to 25 %, biases introduced by the possible presence of helium and heavier nuclei do not exceed the level of the statistical uncertainty. This was chosen after a Monte Carlo study that probed the sensitivity of the analysis to the mass composition depending on the choice of different values of η .

THE MEASUREMENT OF Λ_η

We use events collected between 1 Dec 2004 and 20 Sept 2010. The atmospheric and event-quality cuts applied are identical to those used for the analysis of $\langle X_{\max} \rangle$ and $\text{RMS}(X_{\max})$ [6] yielding 11628 high-quality events. The X_{\max} -distribution of these data is affected by the known geometrical acceptance of the fluorescence telescopes as well as by limitations related to atmospheric light transmission. We use the strategy developed for the measurement of $\langle X_{\max} \rangle$ and $\text{RMS}(X_{\max})$ to extract a sample that has an unbiased X_{\max} -distribution: a fiducial volume selection, which requires event geometries that allow, for each individual shower, the complete observation of a defined slant depth range.

Firstly, we derive the range of values of X_{\max} that corresponds to the fraction $\eta = 0.2$ of the most deeply penetrating showers. For this we need an unbiased distribution of X_{\max} over the entire depth range of observed values of X_{\max} . To achieve this we perform a fiducial event selection of the slant depth range containing 99.8 % of the observed X_{\max} -distribution, which corresponds to the range from 550 to 1004 g/cm². This reduces the data sample to 1635 events providing an unbiased X_{\max} -distribution that is used to find the range of values of X_{\max} corresponding to $\eta = 0.2$, identified to extend from 768 to 1004 g/cm².

Secondly, we select those events from the original 11628 that have geometries allowing the complete observation of values of X_{\max} from 768 to 1004 g/cm², the tail of the unbiased distribution. This fiducial cut maximises the statistics of an unbiased X_{\max} -distribution in the range of interest. In total 3082 events pass the fidu-

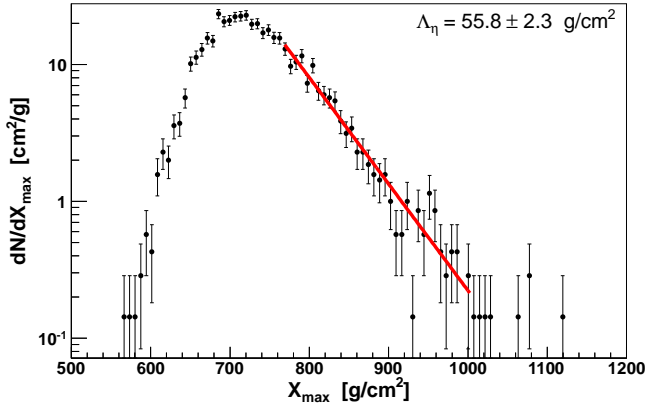


FIG. 1: Unbinned likelihood fit to obtain Λ_η (thick line). The X_{max} -distribution is unbiased by the fiducial geometry selection applied in the range of the fit.

cial volume cuts, of which 783 events have their X_{max} in the selected range and thus contribute directly to the measurement of Λ_η . In Fig. 1 we show the 3082 selected events and the result of an unbinned maximum likelihood fit of an exponential function over the range 768 to 1004 g/cm². Values of Λ_η have been re-calculated for subsamples of the full dataset selected according to zenith-angle, shower-to-telescope distance and energy: the different values obtained for Λ_η are consistent with statistical fluctuations. The re-analyses of the data for changes of fiducial event selection, modified values of η and for different ranges of atmospheric depths yield changes of Λ_η that are distributed around zero with a root-mean-square of 1.6 g/cm². We use this root-mean-square as an estimate of the systematic uncertainties associated to the measurement. This yields

$$\Lambda_\eta = [55.8 \pm 2.3(\text{stat}) \pm 1.6(\text{sys})] \text{ g/cm}^2, \quad (1)$$

with the average energy of these events being $10^{18.24} \pm 0.005(\text{stat})$ eV. The differential energy distribution for these events follows a power-law with index -1.9 . The average energy corresponds to a center-of-mass energy of $\sqrt{s} = 57 \pm 0.3(\text{stat})$ TeV in proton-proton collisions.

DETERMINATION OF THE CROSS-SECTION

The determination of the proton-air cross-section for particle production requires the use of air-shower simulations, which inherently introduces some dependence on model assumptions. We emulate the measurement of Λ_η with Monte Carlo simulations to derive predictions of the slope, Λ_η^{MC} . It is known from previous work that the values of Λ_η^{MC} are directly linked to the hadronic cross-sections used in the simulations [2]. Accordingly we can explore the effect of changing cross-sections empirically

by multiplying all hadronic cross-sections input to the simulations by an energy-dependent factor [7]

$$f(E, f_{19}) = 1 + (f_{19} - 1) \frac{\lg(E/10^{15} \text{ eV})}{\lg(10^{19} \text{ eV}/10^{15} \text{ eV})}, \quad (2)$$

where E denotes the shower energy and f_{19} is the factor by which the cross-section is rescaled at 10¹⁹ eV. This factor is unity below 10¹⁵ eV reflecting the fact that measurements of the cross-section at the Tevatron were used to tune the interaction models. This technique of modifying the original predictions of the cross-sections during the simulation process assures a smooth transition from accelerator data up to the energies of our analysis.

For each hadronic interaction model, the value of f_{19} is obtained that reproduces the measured value of Λ_η . The modified cross-section is then deduced by multiplying the original cross-section used in the model by the factor $f(E, f_{19})$ of Eq. (2) using $E = 10^{18.24}$ eV. For the conversion of Λ_η into cross-section, we have used the four high-energy hadronic interaction models commonly adopted for air shower simulations: QGSJet01 [8], QGSJetII.3 [9], SIBYLL 2.1 [10] and EPOS1.99 [11]. While in general no model gives a completely accurate representation of cosmic-ray data in all respects, these have been found to give reasonably good descriptions of many of the main features. **It has been shown [12] that the differences between the models used in the analysis are typically bigger than the variations obtained within one model by parameter variation. Therefore we use the model differences for estimating the systematic model dependence.**

The proton-air cross-sections for particle production derived for QGSJet01, QGSJetII, SIBYLL and EPOS are 523.7, 502.9, 496.7 and 497.7 mb respectively, with the statistical uncertainty for each of these values being 22 mb. The difference of these cross-sections from the original model predictions are < 5 %, with the exception of the result obtained with the SIBYLL model, which is 12 % smaller than the original SIBYLL prediction. We use the maximum deviations derived from using the four models, relative to the average result of 505 mb, to estimate a systematic uncertainty of $(-8, +19)$ mb related to the difficulties of modelling high energy interactions. This procedure relies on the coverage of the underlying theoretical uncertainties by the available models. For example diffraction, fragmentation, inelastic intermediate states, nuclear effects, QCD saturation, etc. are all described at different levels using different phenomenological, but self-consistent, approaches in these models. It is thus possible that the true range of the uncertainties for air-shower analyses is larger, but this cannot be estimated with these models. Furthermore, certain features of hadronic particle production, such as the multiplicity, elasticity and pion-charge ratio, have an especially important impact on air shower development [13, 14]; of these we found that only the elasticity can have a relevant impact on Λ_η . The identified systematic uncertainty of

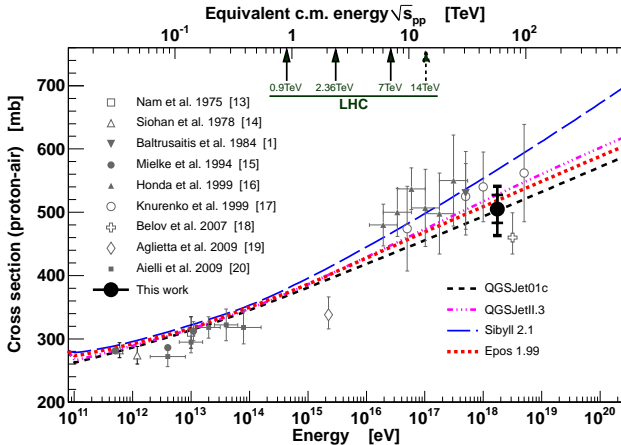


FIG. 2: Resulting $\sigma_{p\text{-air}}^{\text{prod}}$ compared to other measurements (see [16–23] for references) and model predictions. The inner error bars are statistical, while the outer include systematic uncertainties for a helium fraction of 25 % and 10 mb for the systematic uncertainty attributed to the fraction of photons.

($-8, +19$) mb induced by the modelling of hadronic interactions, corresponds to the impact of modifying the elasticity within $\pm(10 - 25)\%$ in the models.

The selection of events with large values of X_{\max} also enhances the fraction of primary cosmic-ray interactions with smaller multiplicities and larger elasticities, which is for example characteristic for diffractive interactions. The value of Λ_η is thus more sensitive to the cross-section of those interactions. The identified model-dependence for the determination of $\sigma_{p\text{-air}}^{\text{prod}}$ is also caused by the compensation of this effect.

Also the choice of a logarithmic energy dependence for the rescaling-factor in Eq. (2) may affect the resulting cross-sections. However, since the required rescaling factors are small, this can only be a marginal effect.

The systematic uncertainty of 22 % [15] in the absolute value of the energy scale leads to systematic uncertainties of 7 mb in the cross-section and 6 TeV in the center-of-mass energy. Furthermore, the procedure to obtain $\sigma_{p\text{-air}}^{\text{prod}}$ from the measured Λ_η depends on additional parameters. By varying the energy distribution, energy and X_{\max} resolution in the simulations, we find that related systematic changes of the value of $\sigma_{p\text{-air}}^{\text{prod}}$ are distributed with a root-mean-square of 7 mb around zero. We use the root-mean-square as estimate of the systematic uncertainties related to the conversion of Λ_η to $\sigma_{p\text{-air}}^{\text{prod}}$.

The presence of photons in the primary beam would bias the measurement. The average X_{\max} of showers produced by photons at the energies of interest is about 50 g/cm² deeper in the atmosphere than that of protons. However, observational limits on the fraction of photons are < 0.5 % [24, 25]. With simulations we find that the possible under-estimation of the cross-section if photons were present in the data sample at this level is less than

10 mb.

With the present limitations of observations, we cannot distinguish air showers produced by helium nuclei from those created by protons. From simulations we find that $\sigma_{p\text{-air}}^{\text{prod}}$ is over-estimated depending on the percentages of helium in the data sample. Lack of knowledge of the helium fraction is the dominant source of systematic uncertainty.

We also find that the nuclei of the CNO-group introduce no bias for fractions up to $\sim 50\%$, and accordingly we assign no uncertainty in the cross-section due to these or heavier nuclei.

In Table I we list the sources of systematic uncertainties. As the helium fraction is not known we show the impact of 10, 25 and 50 % of helium respectively. In what follows we include a systematic uncertainty related to a helium fraction of 25 %. In the extreme case, were the cosmic-ray composition to be 100 % helium, the analysis would over-estimate the proton-air cross-section by 300 to 500 mb. Given the constraints from accelerator data at lower energies and typical model assumptions, this extreme scenario is not realistic.

We summarise our results by averaging the four values of the cross-section obtained with the hadronic interaction models to give

$$\sigma_{p\text{-air}}^{\text{prod}} = [505 \pm 22(\text{stat})^{+28}_{-36}(\text{sys})] \text{ mb}$$

at a center-of-mass energy of $[57 \pm 0.3(\text{stat}) \pm 6(\text{sys})] \text{ TeV}$. In Fig. 2 we compare this result with model predictions and other measurements. The measurements at the highest energies are: HiRes [21] and Fly's eye [2] that are both based on X_{\max} , Yakutsk Array [20] using Cherenkov observations and Akeno [19] measuring electron and muon numbers at ground level. All these analyses assume a pure proton composition. In the context of a possible mixed-mass cosmic-ray composition, this can lead to large systematic effects. Also all these analyses are based on a single interaction model for describing air showers: Only HiRes uses a second model for systematic checks.

TABLE I: Summary of the systematic uncertainties.

Description	Impact on $\sigma_{p\text{-air}}^{\text{prod}}$
Λ_η systematics	± 15 mb
Hadronic interaction models	$+19$ mb -8 mb
Energy scale	± 7 mb
Conversion of Λ_η to $\sigma_{p\text{-air}}^{\text{prod}}$	± 7 mb
Photons, <0.5 %	< +10 mb
Helium, 10 %	-12 mb
Helium, 25 %	-30 mb
Helium, 50 %	-80 mb
Total (25 % helium)	-36 mb, +28 mb

It is one of the prime aims of our analysis to have the smallest possible sensitivity to a non-proton component, and to perform a detailed systematic analysis on the uncertainties related to the mass composition. We also use, for the first time, all hadronic interaction models currently available for the estimation of model-related systematic effects. Furthermore, by using Eq. (2) we derive a cross-section corresponding to a smooth interpolation from the Tevatron measurement to our analysis, with no inconsistencies as in earlier approaches.

COMPARISON WITH ACCELERATOR DATA

For the purpose of making comparisons with accelerator data we calculate the inelastic and total proton-proton cross-sections using the Glauber model. We use standard Glauber formalism [26], extended by a two-channel implementation of inelastic intermediate states [8] to account for diffraction dissociation [27]. The first channel corresponds to $p \rightarrow p$ scattering and has an amplitude of Γ_{pp} , while the amplitude for the other channel is $\Gamma_{pp^*} = \lambda \Gamma_{pp}$ and corresponds to the excitation of a short lived intermediate state. The parameter λ is related to the ratio of single-diffractive cross-section and elastic cross-section. We use a value of $\lambda = 0.5 \pm 0.15$ that is determined from measurements of the single-diffractive cross-section, as well as from proton-carbon cross-section data at lower energies.

This Glauber calculation is model-dependent since neither the parameters nor the physical processes involved are known accurately at cosmic-ray energies. In particular, this applies to the elastic slope parameter, B_{el} , (de-

fined by $d\sigma_{\text{el}}/dt \propto \exp(-|t|B_{\text{el}})$ for very small t), the correlation of B_{el} to the cross-section, and the cross-section for diffractive dissociation. For the example of $\sigma_{pp}^{\text{inel}}$, the correlation of B_{el} with the cross-section is shown in Fig. 3 for $\lambda = 0.5$. We have used the same four hadronic interaction models to determine the uncertainty band of the $B_{\text{el}} - \sigma_{pp}^{\text{inel}}$ correlation. Recent cross-section models such as [28] fall within this band. We find that in the Glauber framework the *inelastic* cross-section is less dependent on model assumptions than the *total* cross-section. The result for the inelastic proton-proton cross-section is

$$\sigma_{pp}^{\text{inel}} = [92 \pm 7(\text{stat})^{+9}_{-11}(\text{sys}) \pm 7(\text{Glauber})] \text{ mb},$$

and the total proton-proton cross-section is

$$\sigma_{pp}^{\text{tot}} = [133 \pm 13(\text{stat})^{+17}_{-20}(\text{sys}) \pm 16(\text{Glauber})] \text{ mb}.$$

The systematic uncertainties for the inelastic and total cross-sections include contributions from the elastic slope parameter, from λ , from the description of the nuclear density profile, and from cross-checking these effects using QGSJetII [9, 29]. For the inelastic case, these three independent contributions are 1, 3, 5, and 4 mb respectively. For the total cross-section, they are 13, 6, 5, and 4 mb. We emphasize that the total theoretical uncertainty of converting the proton-air to a proton-proton cross-section may be larger than estimated here within the Glauber model. There are other extensions of the Glauber model to account for inelastic screening [8, 30] or nucleon-nucleon correlations [31], and alternative approaches that include, for example, parton saturation or other effects [11, 29, 32, 33].

In Fig. 4 we compare our inelastic cross-section result to accelerator data and to the cross-sections used in the hadronic interaction models.

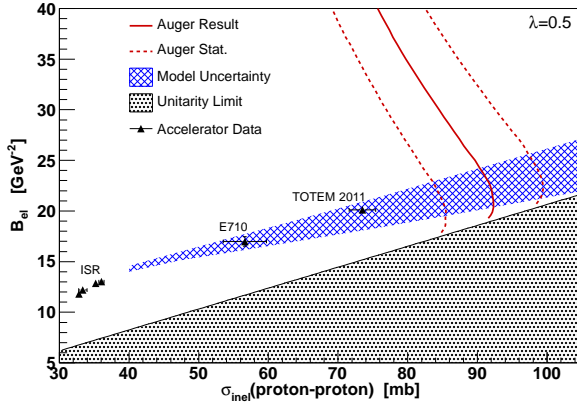


FIG. 3: Correlation of elastic slope parameter, B_{el} , and the inelastic proton-proton cross-section in the Glauber framework. The solid line indicates the parameter combinations yielding the observed proton-air production cross-section, and the dotted lines are the statistical uncertainties. The hatched area corresponds to the predictions by SIBYLL, QGSJet, QGSJetII and EPOS. See also Ref. [5].

SUMMARY

We have presented the first measurement of the cross-section for the production of particles in proton-air collisions from data collected at the Pierre Auger Observatory. We have studied in detail the effects of assumptions on the primary cosmic-ray mass composition, hadronic interaction models, simulation settings and the fiducial volume limits of the telescopes on the final result. By analysing only the most deeply penetrating events we selected a data sample enriched in protons. The results are presented assuming a maximum contamination of 25 % of helium in the light cosmic-ray mass component. The lack of knowledge of the helium component is the largest source of systematic uncertainty. However, for helium fractions up to 25 % the induced bias remains below 6 %.

To derive a value of $\sigma_{p\text{-air}}^{\text{prod}}$ from the measured Λ_η we assume a smooth extrapolation of hadronic cross-sections from accelerator measurements to the energy of the analysis. This is achieved by modifying the model-predictions

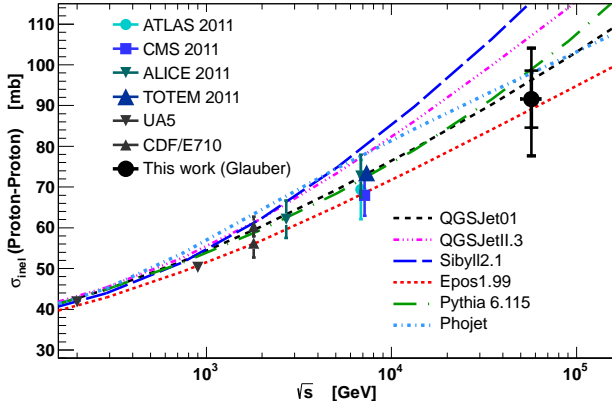


FIG. 4: Comparison of derived σ_{pp}^{inel} to model predictions and accelerator data [34]. Here we also show the cross-sections of two typical high-energy models, Pythia6 [35] and Phojet[36]. The inner error bars are statistical, while the outer include systematic uncertainties.

of hadronic cross-sections above energies of 10^{15} eV during the air-shower simulation process in a self-consistent approach.

We convert the proton-air production cross-section into the total, and the inelastic, proton-proton cross-section using a Glauber calculation that includes intermediate inelastic screening corrections. In this calculation we use the correlation between the elastic slope parameter and the proton-proton cross-sections taken from the interaction models as a constraint. We find that the inelastic proton-proton cross-section depends less on the elastic slope parameter than does the total proton-proton cross-section, and thus the systematic uncertainty of the Glauber calculation for the inelastic result is smaller. The data agree with an extrapolation from LHC [34] energies to 57 TeV for a limited set of models.

Acknowledgments. The successful installation, commissioning, and operation of the Pierre Auger Observatory would not have been possible without the strong commitment and effort from the technical and administrative staff in Malargüe.

We are very grateful to the following agencies and organizations for financial support: Comisión Nacional de Energía Atómica, Fundación Antorchas, Gobierno De La Provincia de Mendoza, Municipalidad de Malargüe, NDM Holdings and Valle Las Leñas, in gratitude for their continuing cooperation over land access, Argentina; the Australian Research Council; Conselho Nacional de Desenvolvimento Científico e Tecnológico (CNPq), Financiadora de Estudos e Projetos (FINEP), Fundação de Amparo à Pesquisa do Estado de Rio de Janeiro (FAPERJ), Fundação de Amparo à Pesquisa do Estado de São Paulo (FAPESP), Ministério de Ciência e Tecnologia (MCT), Brazil; AVCR AV0Z10100502 and AV0Z10100522,

GAAV KJB100100904, MSMT-CR LA08016, LC527, 1M06002, MEB111003, and MSM0021620859, Czech Republic; Centre de Calcul IN2P3/CNRS, Centre National de la Recherche Scientifique (CNRS), Conseil Régional Ile-de-France, Département Physique Nucléaire et Corpusculaire (PNC-IN2P3/CNRS), Département Sciences de l'Univers (SDU-INSU/CNRS), France; Bundesministerium für Bildung und Forschung (BMBF), Deutsche Forschungsgemeinschaft (DFG), Finanzministerium Baden-Württemberg, Helmholtz-Gemeinschaft Deutscher Forschungszentren (HGF), Ministerium für Wissenschaft und Forschung, Nordrhein-Westfalen, Ministerium für Wissenschaft, Forschung und Kunst, Baden-Württemberg, Germany; Istituto Nazionale di Fisica Nucleare (INFN), Ministero dell'Istruzione, dell'Università e della Ricerca (MIUR), Italy; Consejo Nacional de Ciencia y Tecnología (CONACYT), Mexico; Ministerie van Onderwijs, Cultuur en Wetenschap, Nederlandse Organisatie voor Wetenschappelijk Onderzoek (NWO), Stichting voor Fundamenteel Onderzoek der Materie (FOM), Netherlands; Ministry of Science and Higher Education, Grant Nos. N N202 200239 and N N202 207238, Poland; Fundação para a Ciência e a Tecnologia, Portugal; Ministry for Higher Education, Science, and Technology, Slovenian Research Agency, Slovenia; Comunidad de Madrid, Consejería de Educación de la Comunidad de Castilla La Mancha, FEDER funds, Ministerio de Ciencia e Innovación and Consolider-Ingenio 2010 (CPAN), Xunta de Galicia, Spain; Science and Technology Facilities Council, United Kingdom; Department of Energy, Contract Nos. DE-AC02-07CH11359, DE- FR02-04ER41300, National Science Foundation, Grant No. 0450696, The Grainger Foundation USA; ALFA-EC / HELEN, European Union 6th Framework Program, Grant No. MEIF-CT-2005-025057, European Union 7th Framework Program, Grant No. PIEF-GA-2008-220240, and UNESCO.

-
- [1] J. Abraham *et al.*, Nucl. Instrum. Meth. A **523**, 50 (2004).
 - [2] R. Ellsworth *et al.*, Phys. Rev. D **26**, 336 (1982). R. Baltrusaitis *et al.*, Phys. Rev. Lett. **52**, 1380 (1984).
 - [3] P. Sommers, Astropart. Phys. **3**, 349 (1995). B. Dawson *et al.*, Astropart. Phys. **5**, 239 (1996).
 - [4] P. Facal for the Pierre Auger Collaboration and D. Garcia-Pinto for the Pierre Auger Collaboration, 32nd Int. Cosmic Ray Conf., Bejing, arXiv:1107.4804v1 [astro-ph.HE] (2011).
 - [5] R. Engel *et al.*, Phys. Rev. D **58**, 014019 (1998).
 - [6] J. Abraham *et al.*, Phys. Rev. Lett. **104**, 091101 (2010).
 - [7] R. Ulrich *et al.*, New J. Phys. **11**, 065018 (2009).
 - [8] N. Kalmykov and S. Ostapchenko, Phys. Atom. Nucl. **56**, 346 (1993).
 - [9] S. Ostapchenko, Phys. Rev. D **74**, 014026 (2006).
 - [10] E. Ahn *et al.*, Phys. Rev. D **80**, 094003 (2009).

- [11] K. Werner, Phys. Rev. C **74**, 044902 (2006).
- [12] R. Parsons, C. Bleve, S. Ostapchenko, and J. Knapp, Astropart. Phys. **34**, 832 (2011).
- [13] J. Matthews, Astropart. Phys. **22**, 387 (2005).
- [14] R. Ulrich, R. Engel and M. Unger, Phys. Rev. D **83**, 054026 (2011).
- [15] R. Pesce for the Pierre Auger Collaboration, paper 1160, 32nd Int. Cosmic Ray Conf., Bejing, arXiv:1107.4809v1 [astro-ph.HE] (2011).
- [16] R. Nam *et al.*, Proc. of 14th Int. Cosmic Ray Conf., Munich **7**, 2258 (1975).
- [17] F. Siohan *et al.*, J. Phys. G **4**, 1169 (1978).
- [18] H. Mielke *et al.*, J. Phys. G **20**, 637 (1994).
- [19] M. Honda *et al.*, Phys. Rev. Lett. **70**, 525 (1993).
- [20] S. Knurenko *et al.*, Proc. of 26th Int. Cosmic Ray Conf., Salt Lake City **1**, 372 (1999).
- [21] K. Belov *et al.*, Nucl. Phys. Proc. Suppl. **151**, 197 (2006).
- [22] M. Aglietta *et al.*, EAS-TOP Collaboration, Phys. Rev. D **79**, 032004 (2009).
- [23] G. Aielli *et al.*, ARGO Collaboration, Phys. Rev. D **80**, 092004 (2009).
- [24] A. Glushkov *et al.*, Phys. Rev. D **82**, 041101 (2010).
- [25] M. Settimi for the Pierre Auger Collaboration, paper 0393, 32nd Int. Cosmic Ray Conf., Bejing, arXiv:1107.4804v1 [astro-ph.HE] (2011).
- [26] R. Glauber, Phys. Rev. **100**, 242 (1955). R. Glauber and G. Matthiae, Nucl. Phys. B **21**, 135 (1970).
- [27] M. Good and W. Walker, Phys. Rev. **120**, 1857 (1960).
- [28] M. Block, Phys. Rept. **436**, 71 (2006).
- [29] S. Ostapchenko, Phys. Rev. D **81**, 114028 (2010).
- [30] V. Guzey, M. Strikman, Phys. Lett. B **633**, 245 (2006).
- [31] G. Baym, B. Blattel, L.L. Frankfurt, H. Heiselberg and M. Strikman, Phys. Rev. C **52**, 1604 (1995).
- [32] D.R. Harrington, Phys. Rev. C **67**, 064904 (2003).
- [33] L. Frankfurt, G. Miller, M. Strikman, Phys. Rev. Lett. **71**, 2859 (1993).
- [34] G. Aad *et al.*, ATLAS Collaboration, Nature Commun. **2**, 463 (2011). CMS Collaboration, presentation at DIS workshop, Brookhaven, 2011. ALICE Collaboration, presentation at workshope of “Minimum Bias and Underlying Event Working Group”, CERN, 17.6.2011. G. Antchev *et al.*, Europhys. Lett. **96**, 21002 (2011).
- [35] G. Schuler, T. Sjostrand, Phys. Rev. D **49**, 2257 (1994).
- [36] R. Engel, Z. Phys. C **66**, 203 (1995). R. Engel and J. Ranft, Phys. Rev. D **54**, 4244 (1996).